 0014-4754/95/070710-11$1.50 + 0.20

X-rays from the Sun

C.U. Keller

National Solar Observatory, National Optical Astronomy Observatories, P.O. Box 26732, Tucson (Arizona 85726-6732, USA), Fax + 1 520 318 8278

Abstract. X-ray astronomy began in 1948 with the first detection of X-rays from the Sun. Astronomical X-ray observations need to be performed from high-altitude rockets and satellites because the Earth's atmosphere absorbs X-rays. Currently about 100,000 X-ray sources are known all over the sky. The Sun is by far the strongest source. The outermost solar atmosphere, the corona, emits X-rays due to its high temperature of a few million K. Solar X-ray emission is highly variable. Eruptions lead to variations of the X-ray flux on time scales of minutes. The average X-ray flux varies with the 11-year sunspot cycle by a factor of about 1000. Solar X-rays have a profound influence on the Earth's upper atmosphere.

Key words. X-rays; astronomy; sun; corona; solar magnetic fields; satellites; detectors.

Introduction

X-rays in astronomy

This review covers the consequence to solar astronomy of the discovery of X-rays in 1895 by W. C. Roentgen. Roentgen's discovery had no influence on observational astronomy during the first 50 years because the Earth's atmosphere prevents X-rays from reaching the ground. X-ray astronomy was only possible after the development of rockets that could reach far beyond the heights attained by balloons. Consequently the first solar X-rays were recorded in 1948 by US scientists using a German V-2 rocket.

The Sun was the first celestial object to be studied in X-rays since it is by far the brightest source at those wavelengths. Apart from that, the Sun occupies a particular position among all the other stars. The Sun is the closest star to Earth and is the only star where processes can be studied in great detail. Modern solar telescopes may resolve features as small as 200 km in size on the Sun while even the largest night-time telescope may just barely resolve the disk of close, very large stars. Solar energy is the key ingredient for life on Earth. Furthermore, the Sun provides physical conditions of matter at pressures, densities, and temperatures that cannot be achieved on Earth. It is therefore of high interest to study the Sun as a prototype of a star and investigate its detailed influence on Earth.

Space-based astronomy, i.e. the observations of celestial objects from high-altitude rockets and satellites, has several advantages over traditional ground-based techniques. In the context of this review the main advantage is the possibility to study those parts of the electromagnetic spectrum that cannot be observed from the ground due to atmospheric absorption, such as X-rays, the UV, and certain parts of the infrared. While the visible and near infrared radiation easily passes the atmosphere, the image quality is severely degraded by the turbulent atmosphere. Telescopes in space produce sharper images than equivalent ground-based instruments. Furthermore the sky is very dark in space. Finally, spaced-based instruments may perform continuous patrol observations for years, uninterrupted by the diurnal cycle or clouds.

Unlike in medicine, where X-rays are used primarily as a penetrating light source to make pictures of human body structures, X-rays are studied in astronomy for what they tell about the sources that produce them. X-ray sources are either high-temperature gases exceeding 10^6 K (plasma) or effects involving charged particles having speeds close to the speed of light.

For the understanding of the following sections, a few definitions and units need to be introduced. X-ray radiation in astronomy is often divided into soft and hard X-rays. Soft X-rays range from 0.1 nm to 10 nm, while the hard range extends from about 0.001 to 0.1 nm. A wavelength of 1 nm corresponds to an energy of 1.24 keV. The angular resolution of telescopes is expressed in seconds of arc (arcsec), which corresponds to 1/3600 of a degree. One second of arc corresponds to 725 km on the solar surface. Spectral lines due to atoms are called emission lines when the atoms emit the light and absorption lines when the atoms absorb the light at a specific wavelength interval.

Table. Physical properties of the Sun

Parameter	Value
Age	4.6×10^9 years
Mass	2×10^{30} kg
Radius	6.96×10^8 m
Mean density	1.4×10^3 kg/m^3
Mean distance from Earth	1.5×10^{11} m
Surface gravity	274 m/s^2
Rotation period at equator	26 days
Luminosity	3.9×10^{26} W

Structure of the Sun

The Sun is a regular, rather small star. The table lists its basic parameters. The main chemical elements are hydrogen (90% in numbers of atoms) and helium (10%), all other elements make up about 0.1% and their abundance ratios are similar to those on Earth. There are many excellent books on the Sun in general, e.g. those by Philips[18] and Stix[20].

The interior of the Sun cannot directly be seen. However, the study of seismic waves on the Sun (helioseismology) and the detection of neutrinos confirm the structure of the Sun as predicted by theoretical models. These models indicate a temperature in the center of about 15 million K. At this temperature, together with a high density of 1.6×10^5 kg/m^3, thermonuclear reactions occur. In the core, which extends to 25% of the radius, hydrogen nuclei are fused into helium nuclei. According to Einstein's $E = mc^2$ law, 0.7% of the mass of hydrogen is thereby transformed into energy. Every second 5 million tons are converted into energy (another million tons is lost due to the solar wind every second; see below). This energy is mostly in the form of gamma and X-rays (see Roth in this issue). These high-energy photons slowly diffuse outwards and thereby reduce their energy. If a single photon could be traced from the interior until it leaves the Sun, it would take about 30 million years to do so due to repeated collisions in the dense solar interior. Outside of the core, energy is transported via photons out to about 70% of the solar radius. From there on, energy transport by convection (heat transport by mass flows) is more efficient.

Neutrinos play a key role in current research on the solar interior. Neutrinos are produced during some of the nuclear reactions. They leave the solar core almost unobstructed and reach the Earth within about 8 minutes. Every cm^2 on Earth encounters some 6×10^{10} neutrinos from the Sun in every second. Since the electrically-neutral neutrinos interact very little with regular matter, almost all pass through the Earth without being absorbed and are not easily detected. Neutrino detectors, containing hundreds of tons of detector material, measure typically one solar neutrino per day. The neutino flux predicted by theories is, however, about three times larger than the observed flux. This is known as the solar neutrino problem. While solar models predicting the theoretical neutrino flux might be wrong, it is much more likely that particle physics has an incomplete knowledge of neutrino physics. An extensive treatment of this problem may be found in the book by Bahcall[1].

Most of the solar light we see on Earth comes from the lowest visible layer of the solar atmosphere, the photosphere. It is only a few 100 km thick. Above that is a layer called chromosphere, which is, astonishingly, hotter than the underlying photosphere. While the photospheric temperature is between roughly 4500 and 6500 K, the chromosphere reaches temperatures of up to 25,000 K. Above that, the corona reaches temperatures of a few million K. The outer corona expands into the interplanetary space and slowly cools off. This is also known as the solar wind. In space near Earth, the temperature is still about 150,000 K, however the density is so low that this is not important for the Earth's energy budget.

Magnetic fields play a fundamental role in our understanding of transient phenomena on the Sun. Solar magnetic fields are generated by a so-called dynamo. The electrically conductive plasma is moved around in the convection zone. This motion together with an existing magnetic field generates electric currents. The latter lead to even stronger magnetic fields. Magnetic fields can therefore be amplified by the motion of the plasma material. The theory of magnetohydrodynamics also explains the observed sunspot cycle, which is a variation of the number of sunspots seen on the solar surface. Sunspots coincide with strong magnetic fields. Measurements of the polarity of sunspot magnetic fields show that the 11-year cycle is part of a 22-year magnetic cycle in which the Sun's magnetic field flips polarities every 11 years.

Similar mechanisms produce magnetic fields in the Earth, other stars, and galaxies. In the Sun, the dynamo is thought to be located at the base of the convection zone, while in planets it is located in their cores. In the solar convection zone and in the photosphere, the magnetic fields are bound to go with the motion of the plasma. In the corona, however, the magnetic fields dominate and prescribe the motion of matter. The strength of the Earth's magnetic field is about 10^{-4} Tesla, while in sunspots several 10^{-1} T may be reached. Magnetic fields in the Sun are almost exclusively measured by investigating the Zeeman effect, which describes the splitting and polarization of spectral lines produced by atoms that are in a magnetic field. Except for sunspots, the splitting of the relatively weak magnetic fields is small and normally cannot be detected. The polarization of spectral lines in the presence of magnetic fields, however, is a very sensitive diagnostic for solar magnetic fields. An instrument that records the circular polarization in a Zeeman sensitive line is called a magnetograph. Its product, a magnetogram, is a map of the local amount of magnetic flux on the Sun (see fig. 3).

Phenomena on the solar surface are often divided into active and quiet Sun phenomena. The quiet Sun describes the spherically symmetric properties of a gas ball that are almost constant in time. The active Sun, on the other hand, describes transient phenomena, such as sunspots and flares (chromospheric eruptions), that are due to the Sun's magnetic field. Without its magnetic field, the Sun would be a rather uninteresting star.

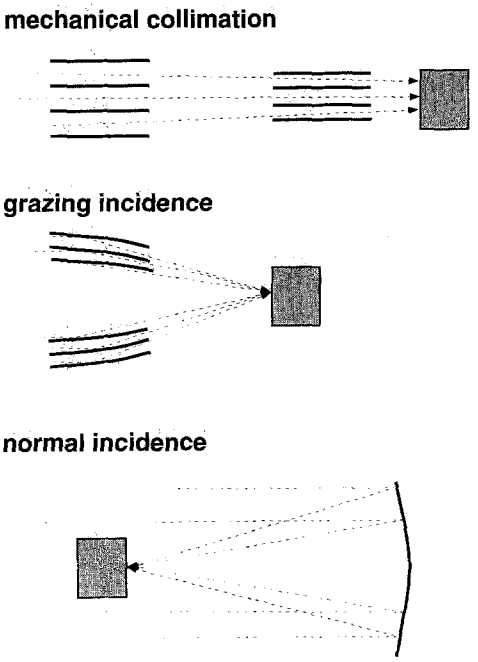

Figure 1. Three different methods to obtain X-ray images of astronomical sources: mechanical collimation: arrangements of X-ray absorbing materials provide a crude imaging capability; grazing incidence: reflection at very shallow angles form an image; normal incidence: reflection at angles almost perpendicular to the reflecting surface focus X-rays.

Astronomical X-ray instrumentation

A large variety of imaging, spectrograph, and detector schemes are employed in astronomical X-ray observations[19]. Here I briefly discuss methods to record X-ray images, spectrometers, and detectors for X-rays used in astromomical instruments.

Image forming devices

While the first astronomical X-ray devices had no imaging capabilities, it became obvious that imaging is needed to study extended sources such as the Sun and to minimize the chances of confusing close sources. Devices that produce an image may be divided into three categories according to their principles.

Mechanical restrictions of the field of view are the oldest technology, but it is still in use at very high energies (wavelengths shorter than 1 nm) where the other methods discussed below do not work. The mechanical restrictions may be as simple as a small hole acting as a pin-hole camera or may consist of elaborate schemes using various grids (see fig. 1).

Grazing incidence optics focus the field of view onto a small detector area similar to optics in the visible light. This method results in a dramatic increase in sensitivity and allows the usage of small, high-performance detectors. Reflective mirror optics, such as used in the visible domain, do not work in X-rays because of the low reflectivity at almost normal incidence. However, reflection at very shallow angles of about 1 degree, i.e. nearly parallel to the optic surface, provides very high reflectivity. This technique requires very accurate figures and smoothness of the surface. The roughness of modern X-ray optics is well below 1 nm rms. The most often used scheme for grazing incidence optics was invented by the German Hans Wolter[24] for X-ray microscopy and employs a two-mirror scheme. To achieve large collection areas, reflective surfaces are nested (see fig. 1).

Soft X-ray telescopes almost exclusively used and still use grazing mirror designs. While these mirrors have a high reflectivity, their total collection area is rather small. The opposite is true for normal-incidence optics, where the collective area is large but the reflectivity is low. Normal incidence describes optics where the beam is almost normal to the optical surfaces. All optics in the visible domain (e.g. photo lenses) are normal-incidence optics. The development of multi-layer optics led to reflectivities of about 10% around 5 nm and up to 50% at 15 nm. These mirrors contain periodic layers of various materials. The thickness of the individual layers is on the order of a few nm. Typically 50 and more layers are used. The drawback of normal-incidence optics is the narrow wavelength region in which they are highly reflective. Typical passbands are 0.1 and 0.2 nm. However, the narrow passbands can simultaneously act as efficient X-ray filters. Different sectors of a mirror may reflect X-rays of different wavelengths. A shutter then selects one of these sectors. Normal incidence optics reach high spatial resolution with modest telescope diameters.

Spectrometers

Spectrometers measure the X-ray intensity as a function of wavelength. Spectroscopy is crucial to determine the physical parameters of X-ray sources. Often these spectra are simple and therefore a relatively simple spectrometer is sufficient to determine source characteristics. There are two main spectrometer types used in astronomical applications: Bragg crystal and grating spectrometers.

Bragg crystal spectrometers are based on interference of the reflections off a crystal lattice. The periodic order of atoms in a crystal leads to a wavelength-dependent reflection angle of the X-rays (Bragg reflection). Another type of spectrometers employs gratings, where a periodic change in reflectivity or transmission leads to similar effects as in crystals. When an X-ray beam falls on a Bragg crystal or a grating, different wavelengths are reflected under different angles. A detector measures the intensity as a function of reflection angle and therefore as a function of wavelength.

Detectors

The general principle of X-ray detection in astronomy lies in the interaction of X-rays with the detector material, which results in free electric charges that are measured. The number of liberated charges contains information on the energy of the detected X-ray photons.

In the case of gas-filled detectors, we may distinguish proportional counters and scintillation detectors. The first are based on the X-ray photon knocking out an electron from the gas (ionization). A high voltage between the front and the back of the detector accelerates the electron. This in turn ionizes further gas atoms (or molecules) and thereby multiplies the single electron in a cascade to a large number of electrons. This charge avalanche is measured when it hits a conducting material that is connected to a measuring device. These conductors may be arrangements of crossed wires that allow position measurements. In gas-scintillation detectors, the X-ray excites but does not ionize the gas atoms or molecules, i.e. the electron is lifted into a higher orbit around the nucleus, but it is not knocked off. The de-excitation of the electron results in UV photons that can then be detected by conventional light detectors.

Microchannel plates, with an inherent advantage of high spatial resolution, are covered with small, densely packed holes. The diameter of the holes is much smaller than their length. As in the case of gas-filled detectors, there is a large electrical voltage difference between the front and back sides of the plate. A special cathode material on top of the multichannel plate provides an X-ray to electron conversion. The electrons are accelerated along the electric potential and knock off electrons when hitting the wall of the holes. This leads again to an avalanche effect.

Charge Coupled Devices (CCD), as used in modern video cameras, are also used to detect X-rays. A CCD consists of an array of single detectors that store the charges liberated by photons from the silicon semiconductor. Modern devices have several million elements. In the optical part of the electromagnetic spectrum every photon generates a single electron. CCDs are, therefore, not sensitive to wavelength in this spectral regime. In the X-ray regime however, each X-ray photon generates several thousand electrons, and the number of electrons is proportional to the energy (or wavelength) of the detected photons. Typically 50 energy bands can be resolved with a modern CCD system.

A brief history of solar X-ray observations

Because radiation below 293 nm is absorbed by the Earth's atmosphere, solar X-ray astronomy was possible only after rockets able to leave the majority of the atmosphere behind were available. For a long time it was not clear at which altitude the UV and X-ray radiations are absorbed. Stratospheric balloons do not reach high enough to significantly extend the solar spectrum towards shorter wavelengths. The first successful spectra of the Sun reaching down to 230 nm were recorded on October 10, 1946 from a V-2 rocket[2] that flew to an altitude of 88 km. The flight followed by many other flights of V-2 rockets flying experiments, designed by the US Naval Research Laboratory (NRL) under the lead of Richard Tousey, extended the solar spectrum down to 200 nm.

The first detection of solar X-rays was made by Burnight on August 5, 1948 using photographic plates with beryllium filters of two different thicknesses[6]. Beryllium is opaque to visible and ultraviolet radiation. The positive identification of X-rays was done by noticing that photosensitive plates with the thinner beryllium filters were blacker than the ones with the thicker filters. The plates were carried to a height of 96 km by an Aerobee high altitude research rocket. Further experiments carried beryllium and aluminum filters with varying thickness. The two elements have different absorption spectra and therefore contain information on the spectrum in the X-ray regime[7]. Most of the observed X-ray energy flux occurred above 0.8 nm. However, on the August 5, 1948 flight, Burnight also detected X-rays below 0.8 nm, which coincided with exceptionally high solar activity. The correlation between X-rays below 1 nm, radio fadeouts, and high solar activity confirmed an old hypothesis that energetic solar radiation disrupts the ionosphere and causes radio short wave fadeouts. Apart from photosensitive emulsions, thermoluminescent phosphors and photon counters were used to detect solar X-rays in the early days of solar X-ray astronomy. These other detectors also detected UV radiation below 200 nm. A recollection of the earlier experiments can be found in the book by Newell[15].

The first X-ray spectrum of the Sun was recorded with a Bragg crystal spectrometer on board a sounding rocket by Blake and coworkers[4] in 1963. The X-ray line spectrum between 1.3 and 2.5 nm showed many emission lines.

High altidude rockets provided observing capabilities only during a few minutes. The development of Earth-orbiting satellites opened a new window to X-ray observations of the Sun. The size and brightness of the Sun was ideal for the early, relatively primitive satellites, and the knowledge of solar energetic radiation was important for the design of adequate protections for astronauts (see Fritz-Niggli in this issue) and for distinguishing nuclear tests from solar events[14]. Sputnik 2 already had electronic counters to measure solar X-rays. Soon, the US also had X-ray sensitive detectors in orbit and took the lead in solar observations from space.

In the following paragraphs I shall discuss some of the major space missions and their scientific highlights.

The Orbiting Geophysical Observatory (OGO) 5 launched in March 1968 monitored solar flares at a high temporal resolution of better than 2.3 seconds in the 0.01 to 0.13 nm range; it used a NaI(Tl) crystal scintillator and a beryllium window as an X-ray filter. Flare observations with OGO-5 revealed that X-ray bursts in

solar flares consist of two components: an impulsive and a slowly varying component each with widely different spectral and temporal characteristics.

A major improvement in X-ray imaging came about with the NASA Skylab mission. Apart from medical and Earth-observing projects, Skylab's solar observatory on the Apollo Telescope Mount was the major scientific project[8, 11]. Among other solar instruments, it carried an X-ray spectrographic telescope built by American Science and Engineering, which imaged the higher corona in a spectral range between 0.2 and 6 nm, and an X-ray telescope built by the Marshall Space Flight Center of NASA and Aerospace Corporation, which imaged the low corona at wavelengths between 0.6 and 3.3 nm. Both telescopes used grazing incidence mirrors and X-ray filters to image the Sun in broad wavelength bands. Furthermore, two additional instruments provided continuous records of the total X-ray flux in the passbands 0.2 to 0.8 nm and 0.8 to 2 nm and a total X-ray monitor that sounded an alarm whenever the X-ray radiation exceeded a certain value. Finally, a hand-held X-ray and extreme ultraviolet camera, built by the US Naval Research Laboratory, could be used by the astronauts during extra-vehicular activity to record the spectra between 1 and 20 nm of selected solar regions. Skylab turned out to be a superb solar observatory, data of which are still analyzed today. Almost a third, 941 man-hours, of the total time Skylab was manned, was spent for solar physics, and 127 047 solar images were recorded on film.

P78-1, launched in 1979 by the US Air Force as part of a space test program, carried two soft X-ray Bragg crystal spectrometers (0.18 to 0.8 nm and 0.55 to 2.5 nm). These instruments provided the first extensive X-ray observations of solar flares at very high spectral resolution[10] of up to 2×10^{-5} nm at 0.2 nm, allowing for the first time detection of the broadening and shift of soft X-ray spectral lines in flares. The X-ray instrumentation of P78-1 used spare parts from NASA's OSO-7 satellite. In addition to the spectrometers, instruments also monitored the total X-ray flux below 0.8 nm and obtained images between 0.3 and 2.5 nm with a spatial resolution of 20 to 60 seconds of arc. It was deliberately destroyed in 1985 in the first successful anti-satellite missile test.

The last major US solar satellite was the Solar Maximum Mission (SMM) launched in early 1980 to study the solar activity near the maximum of its cycle[5]. Most of the instruments were intended to study flares from the visible to gamma rays. It contained among other instruments a soft X-ray spectrometer, a hard X-ray spectrometer, and an imaging spectrometer sensitive to soft and intermediate-energy X-rays. The hard X-ray Burst Spectrometer measured X-rays in 15 channels from 0.005 to 0.06 nm using a CsI(Na) scintillator detector. The hard X-ray imaging spectrometer built by the Space Research Laboratory in the Netherlands and the University of Birmingham used a collimator system with 900 miniature proportional counters to image the Sun at 0.04 to 0.4 nm and thereby reached a spatial resolution down to 8 by 8 arcseconds with a moderate energy resolution of 10 to 20%. The soft X-ray polychromator used two Bragg crystal spectrometer types to monitor emission lines in the 0.14 to 2.24 nm range either with good spatial and temporal resolution or at good spectral and temporal resolution but bad spatial resolution. It thereby covered a temperature range of 1.5 to 50×10^6 K. SMM was successfully repaired in space and continued its mission until late 1989 when the increasing solar activity extended the Earth's atmosphere outwards causing SMM, because of increased drag, to slow down until its reentry.

The Normal Incidence X-ray Telescope (NIXT) built by the Smithsonian Astrophysical Observatory and the IBM Thomas J. Watson Research Center reached a spatial resolution well below one arcsec[13]. It was flown several times on sounding rockets and used a 25 cm Co-C multi-layer mirror that was sensitive at 6.35 nm with a spectral bandwidth of 0.14 nm. In this wavelength region, the solar corona shows emission lines due to Fe XVI and Mg X.

Japanese solar X-ray astronomy began with the Hinotori (Japanese for Phoenix) spacecraft that operated for one and a half years starting early in 1981[21]. Similar to SMM, it was used to study solar flares. Hinotori concentrated on the three axes space, time, and energy. The spacecraft rotated at a constant rate with the spin axis about 1 degree off Sun center. By using a fine grid modulation collimator, that rotated with respect to one or more grids, images in hard X-rays were obtained. Hinotori observed more than 700 flares.

The most advanced solar X-ray satellite is the Japanese Yohkoh (Japanese for sunbeam) spacecraft launched in August 1991. Yohkoh's primary scientific objective is the understanding of solar flares. It carries a hard and a soft X-ray imaging telescope along with a Bragg crystal and a wide-band spectrometer[16]. The grazing incidence Soft X-ray Telescope uses a 1024 by 1024 elements CCD detector to record X-rays or visible light images with a lens in the center of the X-ray optics. It reaches a resolution of 2.5 arcsec and uses 5 different X-ray filters to observe in various bands in the 0.3 to 4.5 nm wavelength range. The images in figure 3 were obtained with this telescope. The Hard X-ray Telescope uses 64 mechanical collimators to obtain images of the full solar disk with a resolution of about 5 arcsec. It operates in four bands within the 0.01 to 0.08 nm range. Yohkoh observations show the outer corona out to one solar radius, the slow eruption of loops in active regions, coronal mass ejections and jets in X-rays, flares on very small scales (microflares), impulsive foot-point bright-

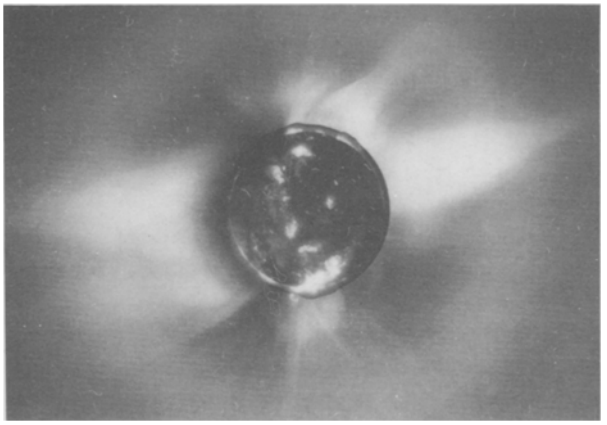

Figure 2. An image of the solar corona recorded during the July 11, 1991 eclipse. It is a composite showing the eclipse picture recorded in white light on Mauna Kea (Hawaii) by Serge Koutchmy and superimposed on the lunar disk a soft X-ray picture obtained simultaneously at 6.4 nm during a NIXT rocket flight from White Sands (New Mexico, USA) by Leon Golub. Courtesy Serge Koutchmy.

ening during flares, bright tops of flare loops, and very hot sources during flares of up to 20 million degrees.

Many satellites with primary goals other than solar physics carry small solar X-ray instruments. The US Geostationary Operational Environment Satellites GOES 6 and 7 and the USSR geophysical research satellite PROGNOZ 9 use broad-band channel full-disk detectors that allow a rough discrimination between soft and harder X-rays. From these long-lasting instruments, it was deduced that during a solar cycle about 10 flares reach temperatures higher than 30 million K to as high as 50 million K.

The USSR PHOBOS Mars spacecraft also contained solar X-ray instruments. PHOBOS 1 carried a soft X-ray telescope, but before the first images were taken, this spacecraft was lost by a controller failure. PHOBOS 2, which reached Mars, carried soft X-ray photometers operating successfully in two channels at 0.15 to 0.31 nm and at 0.31 to 0.62 nm.

The Ulysses spacecraft of the European Space Agency (ESA) currently is flying over the south pole of the Sun and will later-on also pass over the Sun's north pole, regions that have never been explored before. Its Solar Flare X-ray and Cosmic Gamma Ray Burst Experiment measures the total X-ray flux in the 0.08 to 0. 25 nm range with silicon solid state detectors and in the 0.008 to 0.08 nm range with a CsI detector. To study X-ray bursts, it has a high time resolution of up to 8 ms.

X-ray from the solar corona

Observations of the corona

When the Moon covers the solar disk during a total eclipse, the outermost component of the solar atmosphere, the corona, becomes visible (see fig. 2), a region of the solar atmosphere that is not visible outside of eclipses due to stray-light from the solar disk. However, for observing the corona, total eclipses have the disadvantage of a limited period of only a few minutes. The period can be extended by observing along the totality path either with different instruments or by carrying instruments in a fast aircraft. Furthermore, an eclipse does not reveal the three-dimensional structure of the corona, but only a two-dimensional projection against an imaginary screen of the sky.

The corona is about one million times fainter than the solar disk. The clearest sky on Earth is still about ten times brighter. In the summer of 1930, a Frenchman, Bernard Lyot, used an occulting disk as an artificial moon; taking extreme care of stray-light enabled him to see the corona for the first time outside of a total eclipse. Since regular telescopes produce too much scattered light, Lyot used a single lens and an aperture stop at an image of the primary objective to minimize stray-light. The coronagraph was born. The clear sky on Pic du Midi in the French Pyrenees was also fundamental for Lyot's success. Modern coronagraphs are located on high mountains and mostly observe emission lines (see below). Other instruments also observe the continuous light scattered by electrons in the corona. Coronagraphs are also operated on aircrafts, balloons, and satellites.

The first coronal spectra, obtained by Charles Young and William Harkness on August 7, 1869 during an eclipse, showed a green emission line. When Lyot attached a spectrograph to his coronograph, he instantly discovered new emission lines apart from the green line. Some people attributed these emission lines to a new chemical elememt, that was appropriately called coronium.

The origin of the coronal emission lines remained a puzzle until 15 of the 19 observed coronal emission lines were identified by the Swedish Bengt Edlén in 1941 as forbidden transitions of highly ionized atoms, indicating temperatures in the corona of a few million K and a very low density. Even today it is not clear why the corona is so hot, i.e. what heats the corona. Two of the lines were already identified by the German Walter Grotrian in 1937, but Grotrian was rather sceptical about his own results and did not publish them until 1939. The brightest coronal line, the green line at 530.294 nm is due to Fe XIV, iron atoms that have been stripped of 13 electrons. Apart from lines of Fe XIII, XI, XIV, X, XV, other lines are due to Ca XII, XIII, XV, and Ni XVI, XII, XIII, and XV. The red Fe X and the green Fe XIV lines can be observed over much of the corona and indicate a temperature of about 2 million K. The yellow line at 569.45 nm of Ca XV is only intense over sunspot regions and indicates temperatures of about 4 million K there. Extensive observations of the emission line corona were carried out in Switzerland by Waldmeier[22] covering a full solar cycle.

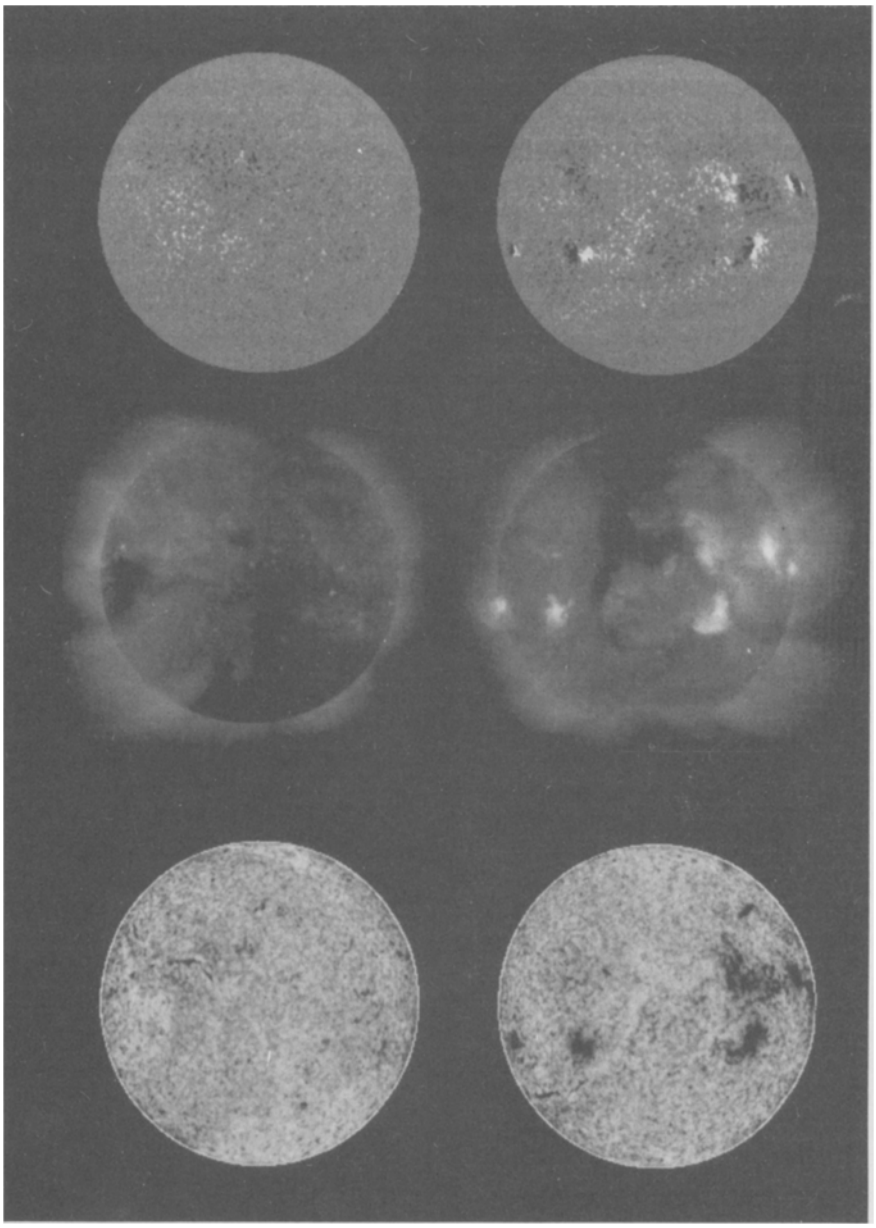

Figure 3. The Sun in a quiet and an active phase. By chance two sides of the solar surface varied greatly in activity in June 1994. The images were taken 12 days apart. The top row shows the Kitt Peak/National Solar Observatory daily magnetograms. Black and white indicate opposite magnetic polarities while gray corresponds to zero magnetic field. The center row shows the simultaneous X-ray images at a mean wavelength of 2 nm. The solar X-ray images are from the Yohkoh mission of ISAS, Japan. The X-ray telescope was prepared by the Lockheed Palo Alto Research Laboratory, the National Astronomical Observatory of Japan, and the University of Tokyo with the suport of NASA and ISAS. The bottom row shows the solar disk in the light of helium at 1083 nm as recorded daily at the National Solar Observatory on Kitt Peak.

In contrast to observations in the visible part of the electromagnetic spectrum, the corona as seen in X-rays can be detected all over the disk, since the lower atmospheric layers do not normally contribute to the X-ray flux. X-ray images are, therefore, fundamental for our understanding of the three-dimensional structure of the corona. X-rays show the inner part of the corona out to about one solar radius. Visible-light coronagraphs in space may detect the corona out to many solar radii.

Lines of highly excited atoms are not only found in the visible and ultraviolet parts of the spectrum, but also in the soft X-ray regime, e.g. Mg XI. These lines are not particularly strong since the energies required to form these emission lines are much larger than the equivalent temperature. These lines are, therefore, sensitive to temperature, while other X-ray lines are sensitive indicators of density.

The solar corona (or hot gas in general) can also be seen in radio waves. In fact, the corona is the main source of solar radio emission at wavelengths longer

than 10 cm. Radio observations also show the corona on the solar disk, however, the spatial resolution of radio observations is much lower and the generation of the radio waves is much harder to interpret as compared to soft X-rays.

Structure of the corona

The corona that is seen during an eclipse is mostly due to scattering of light from the photosphere and chromosphere off electrons and dust. Since emission line intensities are proportional to the electron density squared and the dependence on the temperature is comparatively weak, structures seen in the inner corona with electron densities larger by up to a factor of 20 than the surrounding are easily seen in coronagraphs.

Soft X-ray images of the Sun (see fig. 3) reveal three distinct types of regions: 1) bright regions where closed magnetic fields form so-called coronal loops, arcades, and helmets, which outline the magnetic field lines in the corona, 2) dark regions where the magnetic field lines extend far out from the Sun, before they close; these are called coronal holes and are where the solar plasma flows out to produce the solar wind, 3) and finally the small X-ray bright points that may be found all over the solar disk.

If the corona is heated by thermal processes (e.g. radiation, heat conduction), it could not be hotter than the photosphere which has a temperature of about 5500 K. The corona, therefore, must be heated by non-thermal processes. The problem of coronal heating is far from a satisfactory solution. Several mechanisms have been proposed: acoustic waves, magnetic and magnetohydrodynamic waves, electric currents, reconnection of opposite polarity magnetic fields, very small flares, or combinations of these processes. None of these mechanisms are clearly identified by observations nor in theoretical simulations to explain all the observed properties of the corona. This is not just a solar problem, since almost all stars have outer layers that are hotter than the underlying photosphere.

Coronal holes and the solar wind

Dark coronal holes were discovered by Waldmeier in 1957 using coronal maps constructed from limb observations in the green line[23]. Coronal holes on the solar disk were noted in X-ray pictures made from rockets, but only the Skylab mission clearly showed their structure and evolution. They may also be seen in the extreme ultraviolet and to a certain degree in ground-based observations of the HeI line at 1083 nm (see fig. 3) and in radio maps. Coronal holes are easily detected in X-rays because of the unusually low temperature of about 1×10^6 K and low density. Less than 20% of the solar surface is covered with coronal holes.

At first sight voids in the corona might look rather uninteresting. However, these voids are locations where the magnetic field lines extend into the interplanetary space and permit the free outflow of solar material. Coronal holes are the source of the high-speed stream of solar wind particles that buffet the upper atmosphere of the Earth, disrupting its magnetic field, and producing other lower atmospheric phenomena.

The connection between the solar corona and the interplanetary space was largely ignored until Biermann noticed in 1951 that many comets showed excess ionization and abrupt changes in the material flowing out in the tail that could only be explained by a particle outflow from the Sun[3]. A theoretical investigation of the structure of the corona by Parker [17] showed that there must be a constant outflow from the solar corona due to the high temperature driven by an as yet unknown heating mechanism. As is well known, the existence of the solar wind was indeed confirmed by satellite measurements. Its typical velocity at Earth is about 300 km/s. While it is known that the source of high speed streams of up to 700 km/s are coronal holes, the exact source of the general solar wind is still a matter of discussion.

The active corona

The active corona consists of large, bright active region loops, X-ray bright points, and the transient flares.

In active regions, the magnetic field lines connect photospheric magnetic fields of opposite magnetic polarity. The loops are seen in emission lines at the limb with coronagraphs and in X-rays on the disk. The plasma nicely outlines the magnetic fields lines, since the magnetic field dominates the plasma in the corona (see fig. 3).

X-ray bright points are compact, bright points that can be found all over the Sun. They occur in coronal holes as well as in closed magnetic field regions. They were discovered with rocket flights, but they were far better studied from Skylab. Their lifetimes range from a few hours to several days. At the photospheric level these X-ray bright points correspond to small magnetic regions where two opposite polarity magnetic fields are close by. In X-rays, they seem to consist of many miniature coronal loops.

The most dramatic features that can be seen in X-rays are flares. These explosive events are the most powerful of all forms of solar activity and are one of the most important in terrestrial effects (see below). The total solar X-ray flux changes by up to a factor of a million during a flare. The sudden release of energy can be seen over a large range of the electromagnetic spectrum, from gamma rays to radio waves. The electromagnetic radiation is accompanied by mass motions, particle accelerations, waves, and shocks. Flares are chromospheric eruptions that can be easily seen from the ground in the light of hydrogen (see fig. 4). Some flares are so energetic that they can even be seen in white light. The brightness increases during several minutes and is followed by a

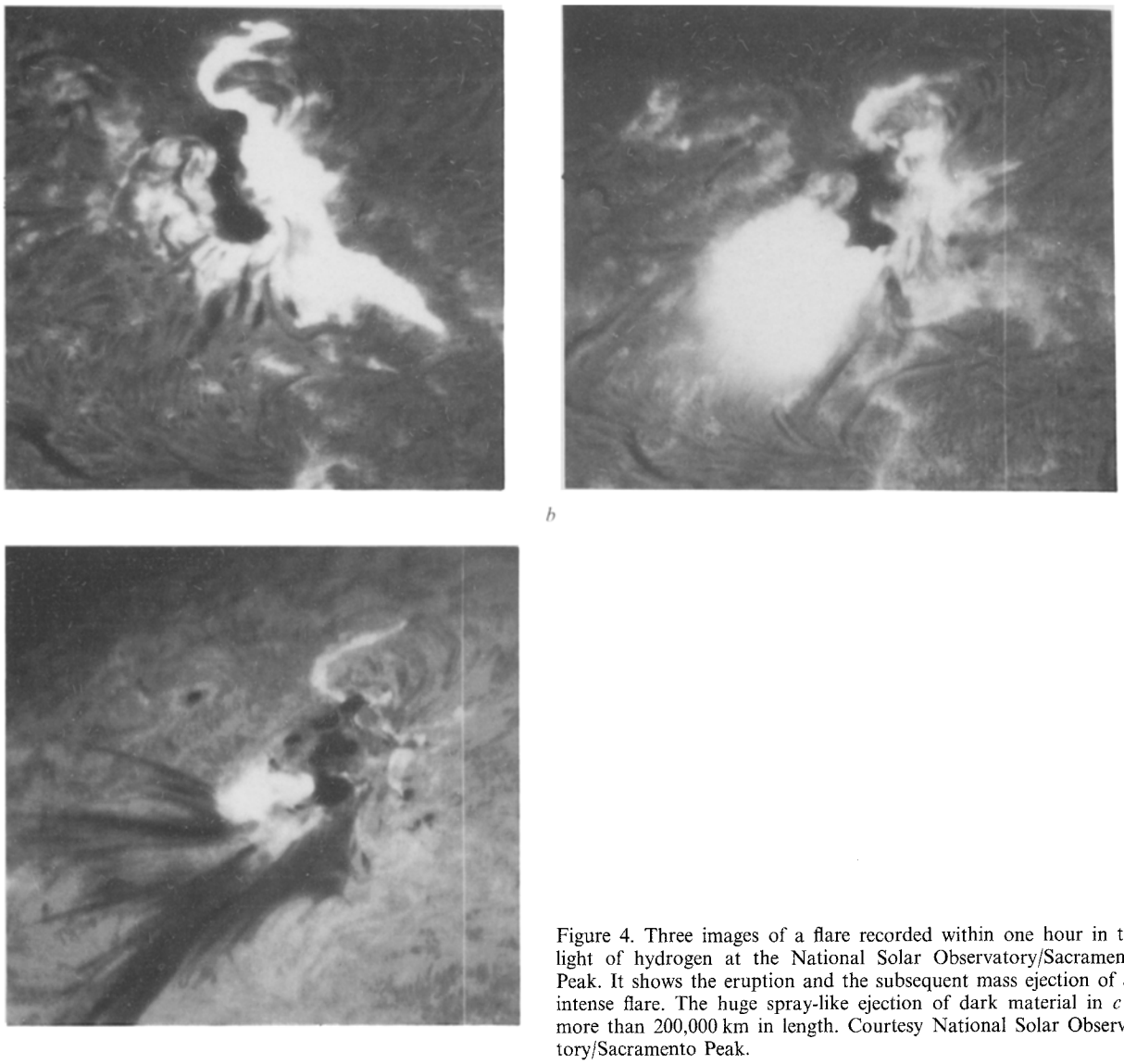

Figure 4. Three images of a flare recorded within one hour in the light of hydrogen at the National Solar Observatory/Sacramento Peak. It shows the eruption and the subsequent mass ejection of an intense flare. The huge spray-like ejection of dark material in *c* is more than 200,000 km in length. Courtesy National Solar Observatory/Sacramento Peak.

slow decay lasting 0.5–1 hours. Electrons at very high speeds produce intense hard X-ray bursts in the beginning of a flare. These electrons travel along the field lines of a magnetic loop until they are stopped by the dense material at the foot-points of the loop. Similar to the electrons stopped in an X-ray tube they emit X-rays. Radio waves are generated by the electrons that spiral along the magnetic field lines of the loop. Accelerated particles collide with the solar gas and produce gamma radiation. Shortly after the beginning of the flare, the particles are slowed down and produce localized temperatures of up to 40×10^6 K, much hotter than the solar interior. Thereby soft X-rays are emitted.

Flares occur in active regions and are most likely when the active region is rapidly developing. The most probable cause of flares is the reconfiguration of magnetic fields. Since flares are associated with active regions, their frequency of occurrence follows the 11-year sunspot cycle.

Influence of solar X-rays on the Earth

Since X-rays from the Sun are absorbed by the Earth's atmosphere, it may be expected that they have a profound influence on the higher layers of the atmosphere. Solar X-rays and extreme ultraviolet radiation, in fact, are responsible for a large part of the ionization in the ionosphere where free electrons and ions exist between about 50 and 300 km. The principal gases that absorb soft X-rays are molecular and atomic oxygen and molecular nitrogen. The most important application of the ionosphere consists in its ability to reflect short-wave radio waves. Strong X-ray flares may disrupt parts of the ionosphere such that communication is almost impossible during the duration of the flare. As soon as the X-ray flux diminishes, communication is possible again. The much enhanced X-ray flux during flares also increases the number of electrons in the ionosphere due to ionization; this in turn enhances the ionospheric

conductivity and affects the Earth's magnetic field. Since the number of flares varies with the sunspot cycle, many properties of the ionosphere also show an 11-year cycle. The temperature in the upper atmosphere varies by a factor of two between sunspot minimum and maximum due to the large variation in solar extreme ultraviolet and X-ray radiation with the solar cycle, which leads to large density variations at any given height in the Earth's atmosphere.

Solar ultraviolet radiation is primarily responsible for the rise in temperature in the lower atmosphere as well as for the formation of the stratospheric ozone. Oxygen molecules (O_2) are split by solar ultraviolet radiation at wavelengths less than 243 nm into two oxygen atoms. The atomic oxygen may then combine with molecular oxygen to form ozone molecules (O_3). Although the maximum concentration of ozone is only a few parts per million, it totally absorbs solar radiation between 240 and 290 nm and partly absorbs between 290 and 320 nm. Since the solar ultraviolet radiation varies by about 1% during the solar cycle, the Sun has an influence on the ozone content in the stratosphere. However, the recently noticed decline in ozone concentration over Antarctica cannot be attributed solely to the Sun. Human influences are primarily responsible for the decline.

Other effects in the ionosphere are due to particles from the Sun, which are a minor part of the cosmic radiation (radiation of extra-terrestrial origin). Together with galactic cosmic rays, particles from the Sun generate secondary particles in the Earth's atmosphere that may reach the ground, significantly adding to the natural radiation (see Roth and Fritz-Niggli in this issue). The dosage due to all cosmic radiation is about 30% of the total dosage at sea level. At higher altitudes, the dosage due to cosmic radiation increases significantly. Only a small fraction of the cosmic ray induced dosage on the ground is due to solar particles. Solar cosmic rays are, however, of danger to astronauts in space. Solar X-rays do not contribute to the radiation dosage from natural sources, since they are absorbed in the upper atmosphere and do not produce secondary particles that would reach the ground. Galactic cosmic rays, whose effects are detected on Earth, vary by some percent during the solar cycle. Near solar maximum, the enhanced solar magnetic activity and its effects on magnetic fields in the interplanetary space provide a certain degree of shielding from galactic cosmic rays. Galactic cosmic rays are, therefore, more abundant during solar minimum.

Cosmic ray particles are mostly protons and Helium nuclei. On the Sun, they are generated during flares and, when hitting the Earth's atmosphere, lead to aurorae and sometimes complete failure of electric power systems in northern countries. Since particles need hours to days to arrive at Earth (in comparison electromagnetic radiation arrives in about 8 minutes), observations of X-rays (that are generated along with the particles) can be used for predicting enhanced particle fluxes from the Sun.

The solar wind produces only small changes in the Earth's magnetic field, but flares and high velocity streams due to coronal holes can produce giant electric current systems in the magnetosphere; these are referred to as geomagnetic storms.

X-rays from other astronomical sources

For a long time it was thought that the Sun is the only X-ray source in the sky. The totally unexpected discovery of a bright X-ray source by Giacconi and coworkers[1,2], who were looking for fluorescence X-rays produced on the lunar surface by solar X-rays, was a big surprise. The source is now known as Scorpion X-1. Since this discovery, non-solar X-ray astronomy has rapidly developed. Today, all celestial objects ranging from stars to quasars are investigated in X-rays. The first X-ray astronomy satellite UHURU was launched in 1970 and found a large number of X-ray sources in close double star systems involving neutron stars and possibly black holes. The Einstein X-ray satellite launched in 1978 carried the first focusing X-ray telescope and was orders of magnitude more sensitive than earlier missions. This satellite found that many active galaxies and quasars contain a small strong X-ray emitter at their center. These locations are now known as Active Galactic Nuclei, which might contain a black hole. The most advanced X-ray satellite is the German Roentgen satellite (ROSAT) launched in June 1990 in a collaborative effort of Germany, the USA, and the UK. An all-sky survey conducted by the telescope located about 100,000 X-ray sources. ROSAT contains 4 nested mirrors with a maximum diameter of 83 cm and a focal length of 2.4 m.

Although the Sun is the strongest X-ray source in the sky, it is a weak X-ray source when taking into account the much larger distances to the other X-ray sources. Typical astronomical X-ray sources are coronae on other stars, accretion of mass from a large star onto a neutron star or a black hole, supernova remnants, interstellar hot material in galaxies, certain galaxy nuclei, and galaxy clusters with hot inter-cluster material. X-ray bursts observed from some of these sources last about 1–10 s and are believed to be due to thermonuclear flashes on neutron star surfaces and to accretion instabilities.

Apart from discrete X-ray sources, there also is a weak background X-ray radiation covering the whole sky. Such phenomenon is not seen in the visible, ultraviolet, or IR domain of the electromagnetic spectrum. However, a background is detected in the 3 K microwave radiation from the big bang and in gamma-rays due to an as yet unknown process. The X-ray background was

detected in 1962 by Giacconi and co-workers using a suborbital rocket. The radiation is very isotropic (to better than 0.03%). It may be due to intergalactic plasma Bremsstrahlung with temperatures of 20–60 million K or to very distant point sources, i.e. Quasars (Quasi-stellar objects).

Outlook

The most fundamental problem that needs to be solved in the future is finding the coronal heating mechanism or mechanisms. Theories need to be formulated that can be tested by observations, while observations need to reveal features expected from theories and find new phenomena that might transport energy into the upper layers of the solar atmosphere. Among the observational tools to tackle this problem are two major facilities.

The Japanese Solar-B X-ray and visible solar satellite mission is planned for launch early in 2001. The spacecraft will be equipped with a normal incidence X-ray telescope imaging in four soft-X-ray wavelength bands and in the visible, a 60 cm telescope that operates in the visible and measures the vector magnetic field with high spatial resolution, and an imaging extreme UV spectrograph operating at around 25 nm.

The Large Earth-based Solar Telescope (LEST) is a next generation solar telescope with a 2.4 m primary mirror. Its design will allow observations of solar magnetic fields at unprecedented spatial resolution. Since many theories of coronal heating rely on very small-scale processes associated with magnetic fields, the availability of a next generation solar telescope on the ground is crucial. If funding for this international project can be secured, it may deliver the first solar images within a few years.

As far as non-solar X-ray imaging is concerned, two major satellites will be operational by the end of the decade. The US Advanced X-ray Astrophysical Facility (AXAF) contains four nested 1.2 m grazing incidence mirrors with a focal length of 10 m, which will lead to a high spatial resolution of 0.5 arcsec. It contains two imaging detectors based on multi-channel plates and a CCD sensor, respectively. Furthermore, it contains two sets of transmission gratings. The European X-ray Multi-Mirror observatory (XMM) is built by ESA and will contain 3 grazing incidence X-ray telescopes for imaging and spectroscopic applications. XMM will have a larger collective area and will be able to observe shorter wavelengths than AXAF.

Acknowledgments. I thank K. L. Harvey for carefully reading and commenting on the manuscript. This work was supported by the Swiss National Science Foundation under Grant no. 8229-037202, which is gratefully acknowledged. The National Optical Astronomy Observatories are operated by the Association of Universities for Research in Astronomy, Inc. (AURA) under cooperative agreement with the National Science Foundation.

1 Bahcall, J. N., Neutrino Astrophysics. Cambridge University Press, Cambridge 1989.
2 Baum, W. A., Johnson, F. S., Oberly, J. J., Rockwood, C. C., Strain, C. V., and Tousy, R., Solar Ultraviolet Spectrum to 88 Kilometers. Phys. Rev. *70* (1946) 781–782.
3 Biermann, L., Kometenschweife und solare Korpuskularstrahlung. Z. Astrophys. *29* (1951) 274–286.
4 Blake, R. L., Chubb, T. A., Friedman, H., and Unzicker, A. E., Spectral and photometric measurements of solar X-ray emission below 60 Å. Astrophys. J. *142* (1965) 1–12.
5 Bohlin, J. D., Frost, K. J., Burr, P. T., Guha, A. K., and Withbroe, G. L., Solar Maximum Mission. Sol. Physics *65* (1980) 5–14.
6 Burnight, T. R., Soft X-Radiation in the Upper Atmosphere. Phys. Rev. *76* (1949) 165.
7 Burnight, T. R., Ultraviolet Radiation and X-Rays of Solar Origin, in: Physics and Medicine of the Upper Atmosphere, chap. 13. Eds C. S. White and O. O. Benson Jr. University of New Mexico, Albuquerque 1952.
8 Compton, W. D., and Benson, C. D., Living and working in space: A history of Skylab. NASA SP-4208, Washington DC 1983.
9 Culhane, J. L., and Sanford, P. W., X-ray Astonomy. Charles Scribner's Sons, New York 1981.
10 Doschek, G. A., Solar Instruments on the P78-1 spacecraft. Sol. Physics *86* (1983) 9–17.
11 Eddy, J. A., A new sun: The Solar Results From Skylab. NASA SP-402, Washington DC 1979.
12 Giacconi, R., Gursky, H., Paolini, F. R., and Rossi, B. B., Evidence for X Rays From Outside the Solar System. Phys. Rev. Lett. 9 (1962) 439–443.
13 Golub, L., Herant, M., Kalata, K., Lovas, I., Nystrom, G., Pardo, F., Spiller, E., and Wilczynski, J., Sub-arcsecond observations of the solar X-ray corona. Nature *344* (1990) 842–844 1990.
14 Hufbauer, K., Exploring the Sun: Solar Science since Galileo. Johns Hopkins University Press, Baltimore 1991.
15 Newell, H. E., High Altitude Rocket Research. Academic Press Inc., New York 1953.
16 Ogawara, Y., Takano, T., Kato, T., Kosugi, T., Tsuneta, S., Watanabe, T., Kondo, I., and Uchida, Y., The Solar-A Mission: An Overview. Sol. Physics *136* (1991) 1–16.
17 Parker, E. N., Dynamics of the Interplanetary Gas and Magnetic Field. Astrophys. J. *128* (1958) 664–676.
18 Phillips, K. J. H., Guide to the Sun. Cambridge University Press, Cambridge UK 1992.
19 Ramsey, B. D., Austin, R. A., and Decher, R., Instrumentation for X-Ray Astronomy. Space Science Review *69* (1994) 139–204.
20 Stix, M., The Sun: An Introduction. Springer Verlag, Berlin 1989.
21 Tanaka, Y., Introduction to Hinotori. Sol. Physics *86* (1983) 3–6.
22 Waldmeier, M., Die Sonnenkorona I. Birkhäuser, Basel 1951.
23 Waldmeier, M., Die Sonnenkorona II. Birkhäuser, Basel 1957.
24 Wolter, H., Annln Phys. *10* (1952) 94.